Preprints (www.preprints.org) | NOT PEER-REVIEWED | Posted: 13 May 2019 doi:10.20944/preprints201905.0156.v1

Mathematical Analysis of the Coating Process Over a Porous Web Lubricated with Upper Convected Maxwell Fluid

M. Zafar[a,b], Babar Ahmad[c], M. A. Rana[a] and M. Zahid[d]

[a]Department of Mathematics & Statistics, Riphah International University, Islamabad, Pakistan
[b]Department of Basic Sciences, MCS, National University of Sciences and Technology(NUST) Islamabad 44000, Pakistan
[c]Department of Mathematics, COMSATS University Islamabad, Pakistan
[d]Department of Mathematics, COMSATS University of Science and Technology, Abbottabad, Pakistan

Abstract

Present study offers mathematical calculations of the roll-coating procedure lubricated with upper Convected Maxwell Fluid. An incompressible isothermal viscoelastic fluid is considered with roll and the porous web having uniform velocities. By employing Lubrication Approximation Theory, the desired equations of motion for the fluid concerned over porous web are modelled and analyzed. The suction rate on the web and injection rate at the roll surface are anticipated proportionate. Results for velocity profile and pressure gradient are obtained analytically. Fluid parameters of industrial significance i.e. detachment point, pressure, sheet /roll separating force, power contribution and coating thickness are also calculated numerically. Substantial and monotonic increase is witnessed in these quantities with the increase of flow parameters.

Keywords: Convected Maxwell Flow, Roll Coating Analysis, Lubrication Approximation Theory, Numerical Procedures, Porous Web

1. Introduction

In the said procedure a uniform fine liquid layer is deposited onto a substrate. The fluids used for the purpose have generally non-Newtonian properties. The phenomenon had earned healthy reputation during the past few decades owing to its vast application. Thin**,** uniform liquid coatings are produced on surfaces in many industrial processes. This Process includes paper coating, beatification and protection of fabrics or metal with coating materials, photographic films, coated products and magnetic recording. Such operations depend on a large variety of equipment. Among these roll coaters are considered common in use. Applied mathematicians, numerical analyst and modelers have to undergo serious difficulties while developing appropriate algorithms for calculating such flows. This is owing to complex and higher order leading flow equations of non-Newtonian fluids as compared to Navier-Stokes equations. Numerous leading equations of non-Newtonian fluids have been proposed in the literature due to such complicated flows. Some

 doi:10.20944/preprints201905.0156.v1

valuable research in this direction is mentioned in [1, 2]. The use of Pseudo plastic fluids being non-Newtonian, is very common. The study of pseudo plastic fluids has gained significance because of its maximum uses in industry. Emulsion coated sheets like photographic films along with solutions and melts of high molecular weight polymers and polymer sheets extrusion etc. are common examples. Some attention has been given to model of Upper convected fluid model, which displays behavior consistent with pseudo plastic fluids.

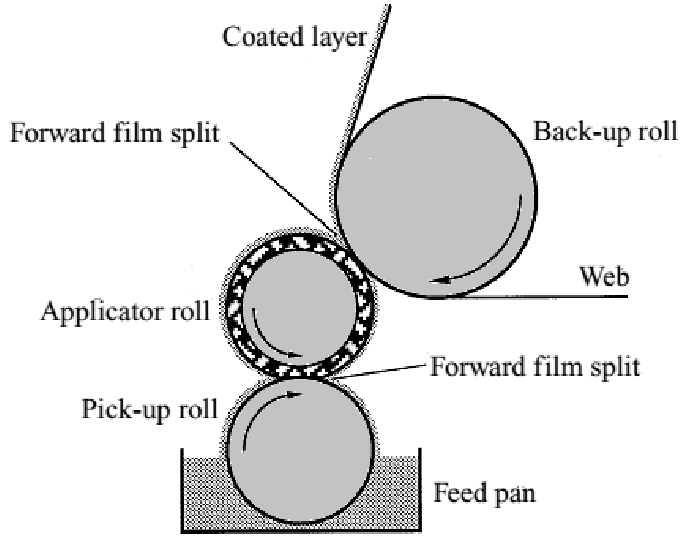

Fig. 1 Sketch of the physical model under study

For better understanding the process, numerous theoretic study have been undertaken by scientists. Taylor and Zettlemoyer[3] employing the lubrication theory studied the flow behavior of ink in a printing press process. Results of pressure distribution and force were derived by them. Flow of water between two rolls was deliberated upon by Hintermaier and White [4] employing the lubrication theory and evaluated the results consistent with their experimental outcomes. Greener and Middleman [5] further attempted to establish the theory of the forward roll coating flow of Newtonian fluids, performing the traditional lubrication approximations along with some simple physical concepts. model of greener and Middleman to a general case of two rollers of equal or non-equalize rotating at equal or non-equal speeds and thereby developing a model which was applicable to general case was studied and improved by Benkreira et al. [6]. The findings of their model were consistent with experimental data. Lubrication Approximation Theory was performed by Souzanna Sofou and Evan Mitsoulis [7] for provision of numerical outcomes in roll coating development over a continuous flat web by using Herschel–Bulkley model of viscoplasticity, which reduces to the Bingham, power-law, and Newtonian models with suitable modifications. Recently M. Zahid et. al. [8] discussed the roll-coating procedure of an incompressible viscoelastic fluid, with roll and the substrate having uniform velocities. Lubrication approximation theory was utilized by them to simplify the conservation equations. Regular perturbation technique was

Preprints (www.preprints.org) | NOT PEER-REVIEWED | Posted: 13 May 2019 doi:10.20944/preprints201905.0156.v1

applied to obtain solutions of velocity profile, pressure gradient, flow rate per unit width, and shear stress at the roll surface.

To our best information, no contribution is available for mathematical formulation of the coating process over porous web with constitutive equations of upper Convected Maxwell Fluid flow. The Aim of this article is to develop the flow process of the coating over porous web of Convected Maxwell Fluid along with investigation of influence of fluid physical properties during the procedure. The article develops as follows. The succeeding sections comprise conservation equations followed by modelling. The coming part covers the analytic expressions of the flow parameters. Lastly findings and discussion along with deductions are presented.

2. Mathematical Formulation

For depositing liquid onto a moving substrate, a laminar, steady flow of an incompressible isothermal upper Convected Maxwell fluid is under consideration. The roll with radius R is rotating anti clock wise with an angular velocity $U = R\omega$. The plane and the roll are moving linearly with the same velocity with H_0 as separation at the nip. During the procedure, the suction velocity v_0 is assumed to remain constant. Moreover $x-axis$ is taken along flow motion whereas $y-axis$ is assumed transversal to the flow direction as depicted by Figure 1. Symmetry of the model is pursued for analysis. The motion of Upper Convected Maxwell fluid model is discussed by following equations:

$$\nabla.\overline{V} = 0, \tag{1}$$

$$\rho\frac{D\overline{V}}{Dt} = -\nabla\overline{p} + \nabla.\overline{\tau}\ , \tag{2}$$

Where $\overline{V}$, ρ , $\frac{D}{Dt}(.) = \frac{\partial}{\partial}(.) + \overline{V}.\nabla(.)$, $\overline{p}$ are velocity ,density, the material derivative and pressure respectively. $\overline{\tau}$ Represents the extra stress tensor for Upper Convected Maxwell fluid model which is given by

$$\overline{\tau} = \mu\frac{\partial\overline{u}}{\partial\overline{y}}\ . \tag{3}$$

The length of curved channel being established by the roll and the plane is too large when comparing with the separation at the nip i.e., $H_0 << R$, thus causing the flow two dimensional. Velocity field is assumed as

$$\overline{V} = [\overline{u}(y), v_0, 0]\ . \tag{4}$$

Preprints (www.preprints.org) | NOT PEER-REVIEWED | Posted: 13 May 2019 doi:10.20944/preprints201905.0156.v1

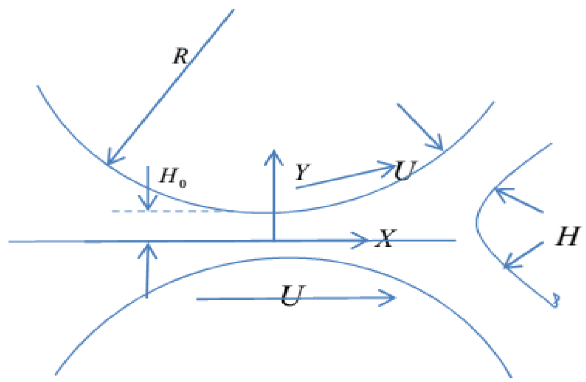

Fig. 2. Mathematical illustration of the region under study

As a result of eq. (4), eqs. (1)- (2) in components form become

$$\frac{\partial \bar{u}}{\partial \bar{x}}+\frac{\partial \bar{v}}{\partial \bar{y}}=0, \tag{5}$$

$$\rho[(\bar{u}\frac{\partial \bar{u}}{\partial \bar{x}}+\bar{v}\frac{\partial \bar{u}}{\partial \bar{y}}+\beta(\bar{u}^2\frac{\partial^2 \bar{u}}{\partial \bar{x}^2}+\bar{v}^2\frac{\partial^2 \bar{u}}{\partial \bar{y}^2}+2\bar{u}\bar{v}\frac{\partial^2 \bar{u}}{\partial \bar{x}\partial \bar{y}})]=-\frac{\partial \bar{p}}{\partial \bar{x}}+\mu(\frac{\partial^2 \bar{u}}{\partial \bar{x}^2}+\frac{\partial^2 \bar{u}}{\partial \bar{y}^2}), \tag{6}$$

$$\rho[(\bar{u}\frac{\partial \bar{v}}{\partial \bar{x}}+\bar{v}\frac{\partial \bar{v}}{\partial \bar{y}}+\beta(\bar{u}^2\frac{\partial^2 \bar{v}}{\partial \bar{x}^2}+\bar{v}^2\frac{\partial^2 \bar{v}}{\partial \bar{y}^2}+2\bar{u}\bar{v}\frac{\partial^2 \bar{v}}{\partial \bar{x}\partial \bar{y}})]=-\frac{\partial \bar{p}}{\partial \bar{y}}+\mu(\frac{\partial^2 \bar{v}}{\partial \bar{x}^2}+\frac{\partial^2 \bar{v}}{\partial \bar{y}^2}), \tag{7}$$

Where β and v_0 represents viscoelastic parameter and suction velocity respectively. Based on the lubrication theory we get

$$\rho v_0\frac{\partial \bar{u}}{\partial \bar{y}}+\rho\beta({v_0}^2\frac{\partial^2 \bar{u}}{\partial \bar{y}^2})=-\frac{\partial \bar{p}}{\partial \bar{x}}+\mu\frac{\partial^2 \bar{u}}{\partial \bar{y}^2}, \tag{8}$$

$$v_0\frac{\partial \bar{u}}{\partial \bar{y}}+\beta({v_0}^2\frac{\partial^2 \bar{u}}{\partial \bar{y}^2})=-\frac{1}{\rho}\frac{\partial \bar{p}}{\partial \bar{x}}+\nu\frac{\partial^2 \bar{u}}{\partial \bar{y}^2}, \tag{9}$$

Where $\nu=\frac{\mu}{\rho}$.

After rearranging eq. (9), we get

Preprints (www.preprints.org) | NOT PEER-REVIEWED | Posted: 13 May 2019 doi:10.20944/preprints201905.0156.v1

$$\frac{\partial \bar{u}}{\partial \bar{y}} + \beta v_0 \frac{\partial^2 \bar{u}}{\partial \bar{y}^2} = -\frac{1}{\rho v_0}\frac{\partial \bar{p}}{\partial \bar{x}} + \frac{\nu}{v_0}\frac{\partial^2 \bar{u}}{\partial \bar{y}^2}, \tag{10}$$

For non-dimensional expressions, introduce variables defined by

$$x = \frac{\bar{x}}{\sqrt{2RH_0}}, y = \frac{\bar{y}}{H_0}, u = \frac{\bar{u}}{U}, p = \frac{H_0 \bar{p}}{\mu U}\sqrt{\frac{H_0}{2R}}, \mathrm{Re} = \frac{v_0 H_0}{\nu}. \tag{11}$$

with the help of eq. (11), eqs. (10) becomes

$$\frac{\partial^2 u}{\partial y^2} - G\frac{\partial u}{\partial y} = S\frac{\partial p}{\partial x}, \tag{12}$$

Where $G = \frac{\mathrm{Re}}{1-B}, S = \frac{1}{1-B}, B = \frac{\beta v_0{}^2}{\nu}$.

Corresponding dimensionless boundary conditions are

$$\left.\begin{aligned} &\frac{\partial u}{\partial y} = 0 \ \text{at} \ y = 0, \\ &u = 1 \ \text{at} \ y = h(x), \end{aligned}\right] \tag{13}$$

Where $h = 1 + \frac{x^2}{2}$.

To evaluate separation point x_s which is unknown, needs two more boundary conditions. At the axis of symmetry, the separation point become stagnation point i.e.

$$u = 0, x = x_s, y = 0. \tag{14}$$

The concluding boundary condition representing a force or pressure balance at the separation point x_s associates the pressure p to the pressure related with surface tension γ

$$\left.\begin{aligned} &p = \frac{-\gamma}{r} \ \text{at} \ x = x_s, \\ &\text{Or} \\ &p = \frac{-H_0}{r}(N_{Ca_2})^{-1} \ \text{at} \ x = x_s, \end{aligned}\right\} \tag{15}$$

The Parameter $N_{Ca_2} = \frac{\mu U}{\gamma}\left(\frac{H}{H_0}\right)^{\frac{1}{2}}$ is a modified capillary number.

Free surface being semicircular as indicative of figure 2, leads to a good assumption

$$\left.\begin{aligned} &2r + 2H = 2H_0 h(x_s), \\ &\text{Or} \\ &\frac{r}{H_0} = h_s - \lambda. \end{aligned}\right\} \tag{16}$$

We know that $h = 1 + \frac{1}{2}x^2$, from this we define

$$h_s = h(x_s) = 1 + \frac{1}{2}{x_s}^2, \tag{17}$$

And

$$\lambda = \frac{H}{H_0}, \tag{18}$$

Where λ is a non-dimensional coating thickness, which is the key parameter that we pursue to calculate through the model.

3. Solution of the Problem

The result of eq. (12) with boundary conditions (13) yields

$$u(y) = \frac{e^{-GH}\frac{dp}{dx}S + e^{Gy}\frac{dp}{dx}S + G(G + \frac{dp}{dx}S(h-y))}{G^2}. \tag{19}$$

$\frac{dp}{dx}$, being part of above equation is still unknown and can be evaluated through introduction of the non-dimensional volumetric flow rate as

$$Q = \lambda = \int_0^h u dy. \tag{20}$$

Insertion of eq. (19) into eq. (20) and subsequent integration yields:

$$\frac{dp}{dx} = \frac{2G^3(\lambda - h)}{S(G^2h^2 - 2Ghe^{Gh} + 2e^{Gh} - 2)}. \tag{21}$$

Since $h(x)$ is an algebraic function, one may integrate eq. (21) to get the pressure profile $p(x)$

$$p(x) = \int_{-\infty}^{x} \frac{2G^3(\lambda - h)}{S(G^2h^2 - 2Ghe^{Gh} + 2e^{Gh} - 2)} dx. \tag{22}$$

By using (15) the expression for λ is obtained, which become

$$p(x_s) = -\frac{1}{(h_s - \lambda)N_{Ca_2}} = \int_{-\infty}^{x_s} \frac{2G^3(\lambda - h)}{S(G^2h^2 - 2Ghe^{Gh} + 2e^{Gh} - 2)} dx. \tag{23}$$

Separation point x_s is still unknown. For this substitute eq. (21) into eq. (19) and use boundary conditions (14) we get

$$\lambda = \frac{1}{4}\frac{G^2 x_s^{\,4} + 4G^2 x_s^{\,2} + 4G x_s^{\,2} + 4G^2 + 8G - 8e^{\frac{1}{2}G(x_s^{\,2}+2)} + 8}{G(G x_s^{\,2} + 2G - 2e^{\frac{1}{2}(x_s^{\,2}+2)} + 2)}. \tag{24}$$

It is quite evident from Fig.2 that the film splitting uniformly, therefore the separation point is $\left(x_s, \frac{1}{2}h\left(x_s\right)\right)$**.** **V**elocity and pressure tend to vanish at this position. The assumption can be agreed to as roll and the sheet moving with the equal velocity. From this explicit relation dimensionless coating thickness λ can be evaluated.

By using eq. (24) into eq. (23), one can use Trapezoidal rule to approximate the complex integral by fixing $B = 10, \mathrm{Re} = 10$ and $N_{Ca_2} = 1$.

B	x_s	λ	F	p_w
1.1	1.8000	1.3050	7.8107	-0.2335
2	1.8425	1.3437	10.3295	-0.3614
3	1.8883	1.3864	13.8451	-0.5327
4	1.9254	1.4218	17.7476	-0.7010
5	1.9567	1.4522	22.0537	-0.8803
6	1.9838	1.4789	26.7183	-0.9980
7	2.0075	1.5025	31.6752	-1.1240
8	2.0282	1.5234	36.8622	-1.2360
9	2.0466	1.5421	42.2522	-1.3367
10	2.0630	1.5590	47.8226	-1.4263

Table 1. Influence of Maxwell parameter on separation point, coating thickness, separating force and power input by fixing $\mathrm{Re} = 10, N_{Ca_2} = 1$

Re	x_s	λ	F	p_w
2	2.2351	1.2027	5.1937	-0.0433
4	2.1744	1.1553	0.8853	0.1910
6	2.1282	1.1203	-2.9233	0.3726
8	2.0919	1.0933	-6.3312	0.4912

Preprints (www.preprints.org) | NOT PEER-REVIEWED | Posted: 13 May 2019 doi:10.20944/preprints201905.0156.v1

10	2.0630	1.0721	-9.4709	0.5914
15	1.9999	1.0271	-17.6440	0.7867
20	1.9774	1.0114	-23.5755	0.8553
30	1.9362	0.9831	-37.1632	0.9527
50	1.8952	0.9556	-65.0365	1.0213
90	1.8612	0.9332	-122.8755	1.0673

Table. 2 Effect of Reynolds Number on separation point, coating thickness, separating force and power input fixing $B=10, N_{Ca_2}=1$

N_{Ca_2}	x_s	λ
1	2.2474	1.2303
2	2.2563	1.2376
3	2.2592	1.2400
4	2.2607	1.2412
5	2.2615	1.2418
6	2.2619	1.2422
7	2.2625	1.2427
8	2.2629	1.2430
9	2.2631	1.2432
10	2.2633	1.2433

Table. 3 Effect of modified capillary number on separation point, coating thickness by fixing $\mathrm{Re}=1$ ***and*** $B=7$

4. Operating Variables

Having calculated the velocity, pressure gradient and pressure distribution, the remaining desired quantities are easily obtained. The operating parameters used for industrial purpose are evaluated as under.

Preprints (www.preprints.org) | NOT PEER-REVIEWED | Posted: 13 May 2019 doi:10.20944/preprints201905.0156.v1

4.1. Separating Force

The roll separating force F is given as

$$F = \int_{-\infty}^{x_s} p(x)dx\,, \tag{25}$$

Where $F = \frac{\bar{F}H_0}{\mu URW}$, $\bar{F}$ is the dimensional roll separating force per unit width W.

4.2. Power Input

The power transferred to the fluid by roll is computed by following integral by setting $\bar{y} = H_0$, as

$$p_w = \int_{-\infty}^{x_s} \tau(x,1)dx\,, \tag{26}$$

Here $p_w = \frac{\bar{p}w}{\mu WU}$ and $\tau_{xy} = \frac{\bar{\tau}_{xy}H_0}{\mu U}$ are the non - dimensionl power and stress tensor given by

$$\tau_{xy} = \frac{\partial u}{\partial y}\,. \tag{27}$$

4.3. Adiabatic Temperature

The temperature of the fluid is raised due to power input by an amount which at most, is given by an adiabatic temperature rise $(\Delta T)_{ave}$

$$(\Delta T)_{ave} = \frac{p_w}{Q\rho C_p}\,, \tag{28}$$

Where ρ, C_p is the melting density and heat capacity respectively at constant pressure.

Results and Discussion

The article analyzes the coating process over porous web for an incompressible isothermal upper convected Maxwell fluid. The Flow equations are simplified by applying Lubrication Approximation Theory. The numerical outcomes of the exiting coating thickness, the separating point x_s, the separating force and the power input are highlighted in Table 1which is generated through variation of B. The maximum coating thickness up to four decimal places is observed which can be as high as 1.5590. Beyond this point by increasing the value of B ,the coating thickness up to four decimal places remains the same. The highest separation point is detected at $B=10$ which is 2.0630.It is observed that thickness of coating increases by increasing B. The minimum thickness of coating has been observed at $B=1.1$,which is 1.1728. It has been observed that by setting or $B \to 0$ no significant change in coating thickness is found. Whereas by setting $B \to \infty$, it has been examined that $\lambda \to 1.3$ as found in the literature by Greener [5] in 1979. It is worth mentioning that with the variation in B one can really control the coating thickness.

Similarly Table 2 and 3 are generated for various values of Re and N_{Ca_2} respectively. As per the dictates of Table 1, by increasing Reynolds number Coating thickness, detachment point and separating force decreases. Whereas, power transferred to fluid by roll increases with the increase of Reynolds number. From Table 2, increase in coating thickness and detachment point is experienced by increasing modified capillary number.

The outcomes for the non - dimensional velocity profile are shown in figures 3 to 12. Velocity profile is highlighted at various positions of the roll coating process through variation of B and Re. Figs. 3 - 7 indicate that the velocity of the fluid increases by increasing B. Figs. 8 - 12 depict that the velocity is decreasing function of the Reynolds number Re. It is highlighted that as the fluid approaches the separation point the viscous behavior of the fluid increases and subsequently beyond this position, the coating on the web will take place due to the dominance of viscous force over elastic force.

The result for the non - dimensional pressure gradient distribution is shown in Figs. 13 and 14 through variation of B and Re. Whereas the effects for the non - dimensional pressure distribution are projected in figs. 15 and 16. It is observed that pressure gradient is increasing function of B and Re. The Pressure distribution is increasing function of B, whereas increase in Re leads to decrease in Pressure distribution.

Conclusion

To derive numerical results of roll coating procedure over a moving flat porous web being fed from an infinite reservoir, lubrication approximation theory was applied for the steady Upper Convected Maxwell fluid.

The main deductions of the current study are appended below:

- The Reynolds number Re provides a procedure to manage coating thickness and separation point.
- Coating thickness, separation region, roll separation force, power input and pressure can be controlled through Reynolds number Re and fluid parameter B being controlling devices.
- Separation force and pressure distribution are decreasing function Re.
- Power input decreases by increasing Re.
- Separating point and coating thickness increases by increasing Capillary number.
- Viscous force having dominant role, causes visible impact on coating thickness, separation force and Power input.
- The outcome of Middleman [5] are retrieved when $B \to 0$ and $\mathrm{Re} \to 0$.
- The nip region demonstrate highest velocity and pressure gradient.

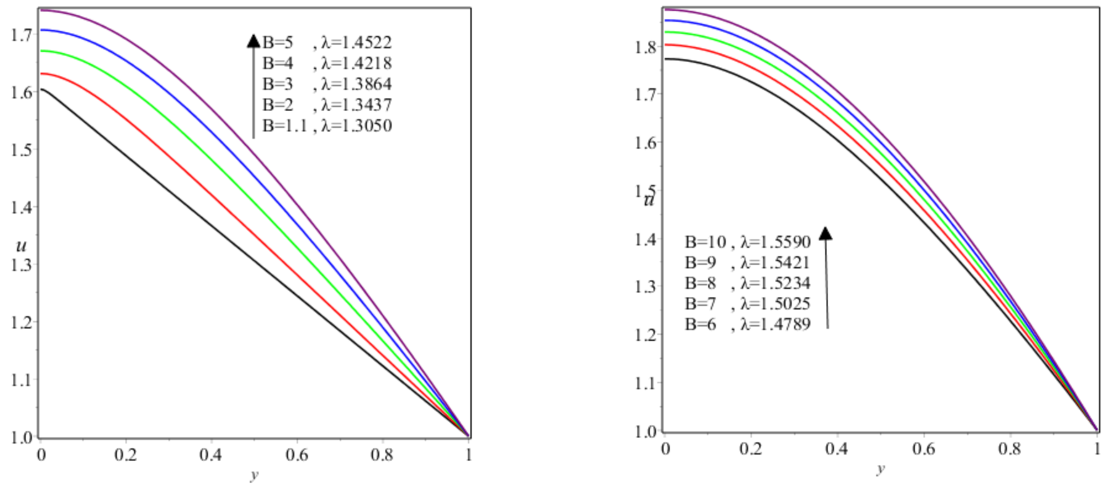

Fig. 3: Influence of B *on velocity profile at* $x = 0$

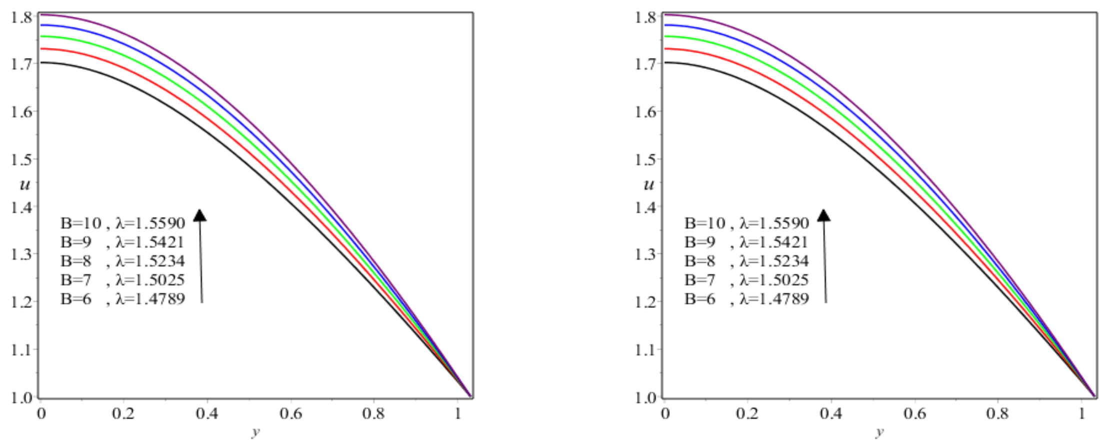

Fig.4: Influence of B *on velocity profile at* $x = 0.25$

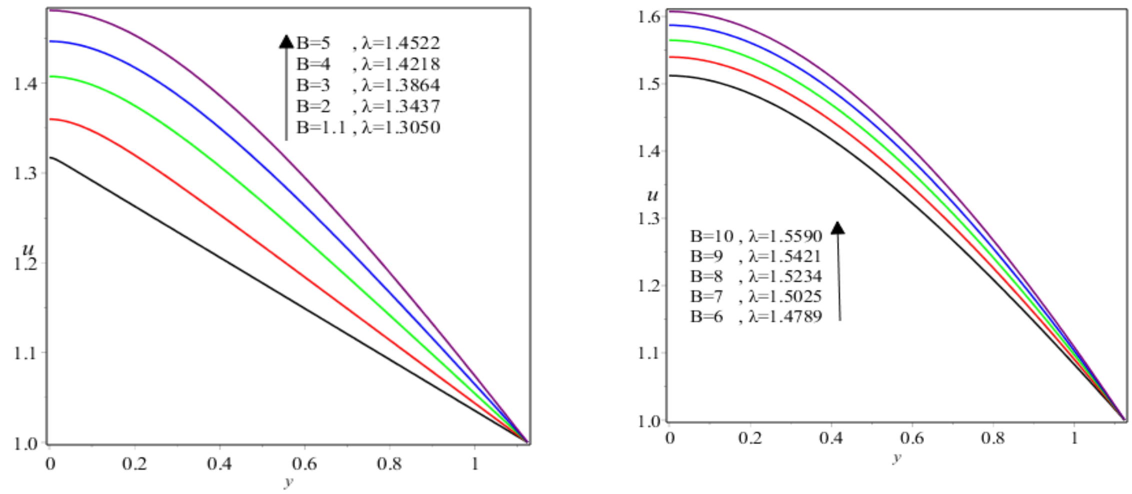

Fig. 5: Influence of B *on velocity profile at* $x = 0.5$

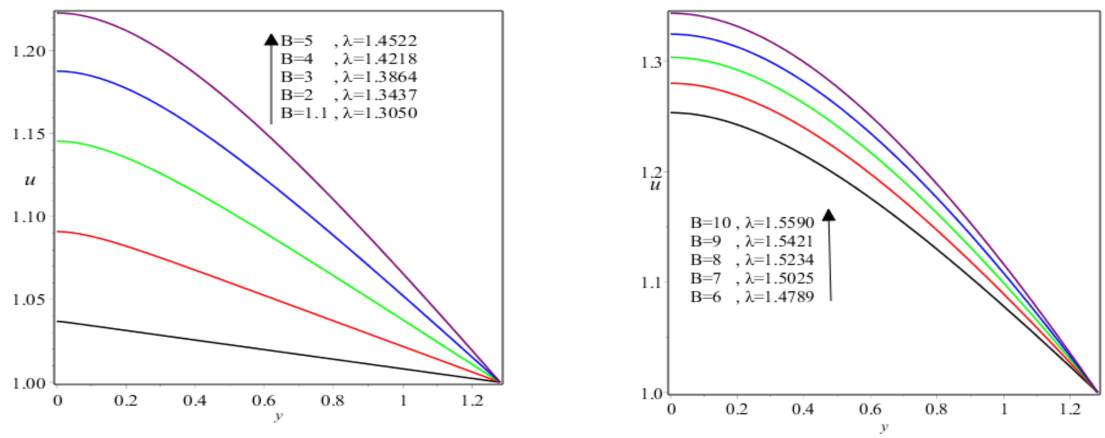

Fig.6: Influence of B *on velocity profile at* $x = 0.75$

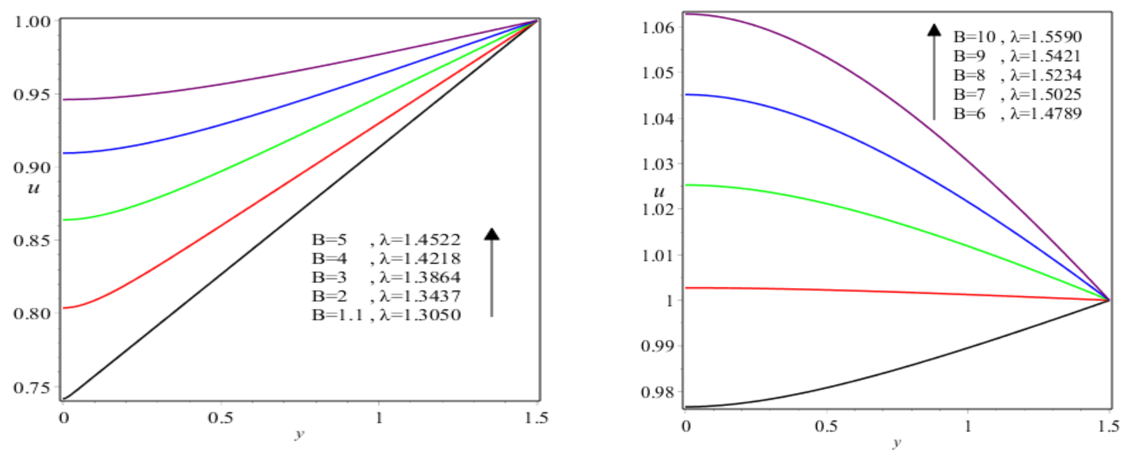

Preprints (www.preprints.org) | NOT PEER-REVIEWED | Posted: 13 May 2019 doi:10.20944/preprints201905.0156.v1

Fig.7: Influence of B *on velocity Profile at* $x = 1$

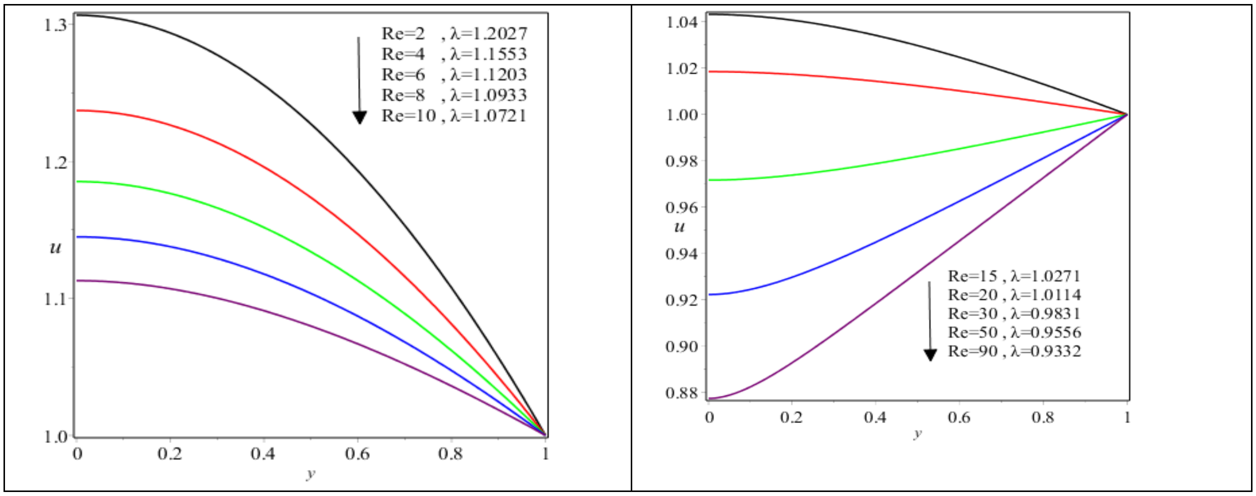

Fig.8:Influence of Re *on velocity Profile at* $x = 0$

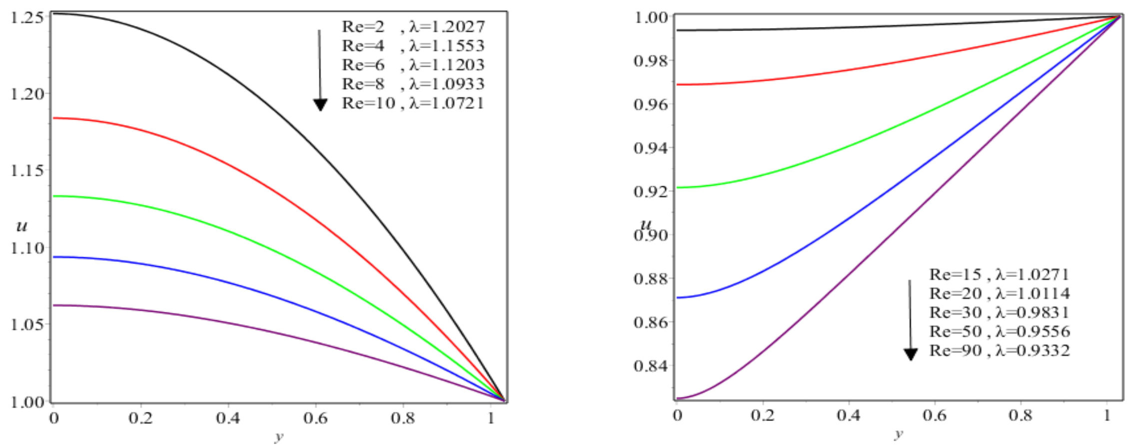

Fig.9: Influence of Re *on velocity profile at* $x = 0.25$

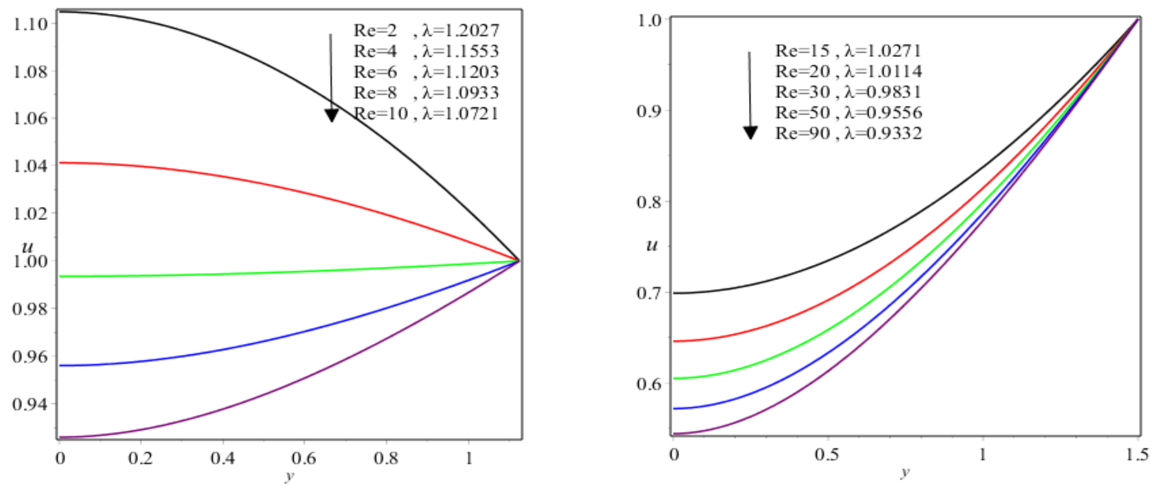

Fig.10: Influence of Re *on velocity profile at* $x = 0.5$

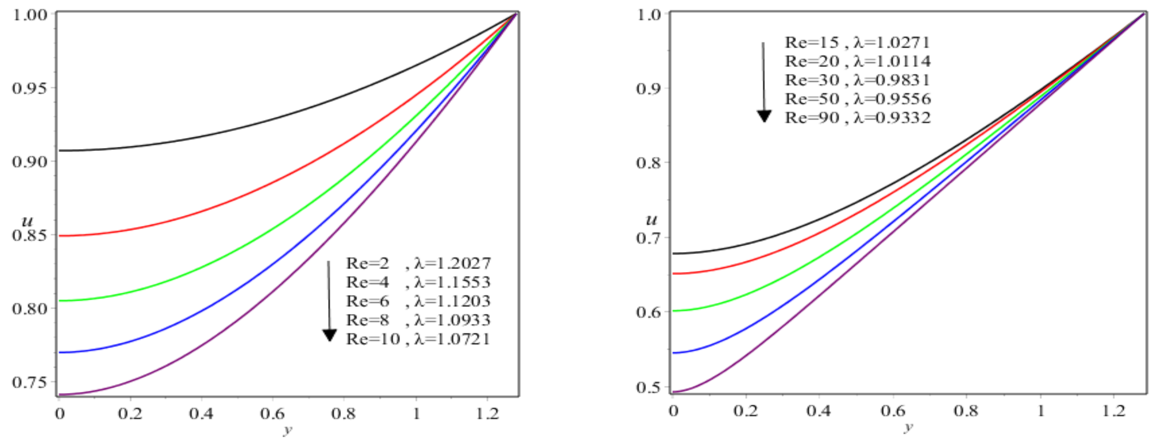

Fig.11: Impact of Re *on velocity profile at* $x = 0.75$

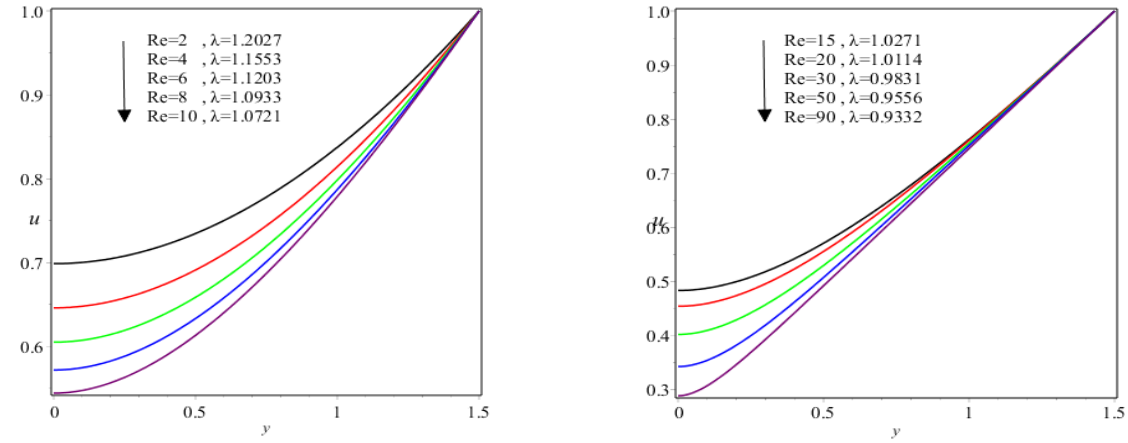

Fig.12: Impact of Re *on velocity profile at* $x=1$

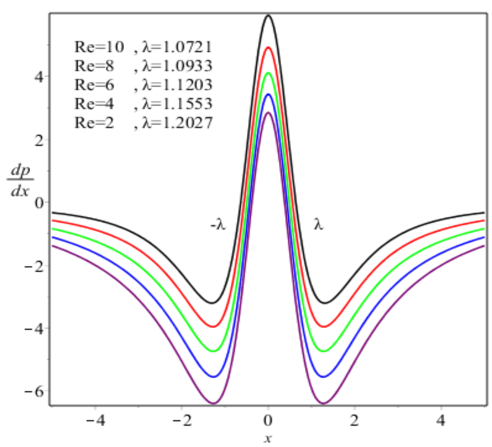

Fig.13: Axial distribution of the pressure gradient by fixing $B=10$

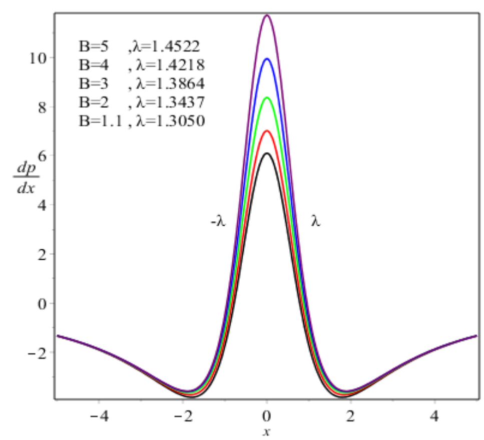

Fig.14: Axial distribution of the pressure gradient by fixing $\mathrm{Re}=10$

Preprints (www.preprints.org) | NOT PEER-REVIEWED | Posted: 13 May 2019 doi:10.20944/preprints201905.0156.v1

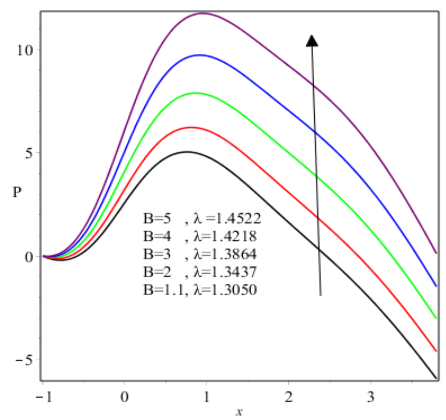

Fig.15: Axial distribution of dimensional pressure fixing $\mathrm{Re} = 10$

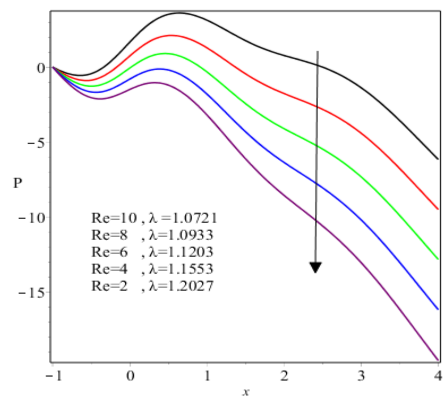

Fig.16: Axial distribution of dimensional pressure by fixing $B = 10$

Reference

1) Rajagopal, K. R.,"A note on unsteady unidirectional flows of a non-Newtonian fluid." Int.J. Non-Linear Mech. 17, pp. 369-373(1982).
2) Benharbit,A.M. and Siddiqui,A.M.,"Certain solution of the equations of the planar motion of a second grade fluid for steady and unsteady cases," Acta Mech. 94,pp.85-96(1992).
3) Taylor,J.H. and Zeltlemoyer,A.C.,"Hypothesis on the mechanism of ink splitting during printing."TAPPI Journal 41, 12,pp.749-757(1958).
4) Hintermaier,J.C. and White,R.E.,"The splitting of a water film between rotating rolls."TAPPI Journal 48,11,pp.617-625(1965).
5) Greener,J. and Middleman, S.,"A theory of roll coating viscous and viscoelastic fluids." Polymer Engineering and Science 15,1,pp.1-10(1975).
6) Benkreira, H., Edwards,M,F. and Wilkinson, W.L.,"A semi-empirical model of the forward roll coating flow of Newtonian fluids,"Chemical engineering Science 42,pp.423-437(1981).
7) Zahid, M., Haroon, T., Rana, M. A., & Siddiqui, A. M. Roll coating analysis of a third grade fluid. Journal of Plastic Film & Sheeting, 33(1), 72-91. (2017).